



OPEN

Precise measurement for line structure light vision sensor with large range

Wei-wei Sheng

High precision and large measurement range are the target of any one three-dimensional scanner. For a line structure light vision sensor, measurement precision depends on its calibration results, i.e., determining mathematical expression of the light plane in camera coordinate system. However, as calibration results are locally optimal solutions, high precise measurement in a large range is difficult. In this paper, we give a precise measurement method and the corresponding calibration procedure for a line structure light vision sensor with a large measurement range. A motorized linear translation stages with a travel range of 150 mm and a planar target which is a surface plate with a machining precision of 0.05 mm are utilized. With the help of the linear translation stage and the planar target, functions which gives the relationship between center point of the laser stripe and the perpendicular/horizontal distance are obtained. Once image of light stripe is captured, we can get a precise measurement result from the normalized feature points. Compared with a traditional measurement method, distortion compensation is not necessary and precision of measurement is improved significantly. Experiments show that root mean square error of measurement results according to our proposed method is reduced by 64.67% related to the traditional method.

A three-dimensional line structure light vision sensor (*LSLVS*) is normally consisted of one image sensor and a line laser projector. It is widely used in the area of industrial measurement owing to its wide measurement range, high precision, easy information extraction and so on. These *LSLVS*s can be classified into two categories according to their construction.

In the first category, the image sensor is a normal camera with a normal lens^{1,2}, i.e. the image plane is parallel to the lens plane. The relationship between image sensor and laser projector is unchangeable and triangulate in the process of measurement. Spatial points can be confirmed once the relationship is determined, which is known as calibration of *LSLVS*.

Heretofore, there are many calibration methods for *LSLVS*. These methods can be classified into three categories according to the ways of obtaining feature points on the laser plane: 3D target based method, planar target based method and 1D target based method³.

In the 3D target based method, geometrical features have been widely used in recent years. Xiao et al.⁴ used an additional facility to control the 3D target, i.e. a very precisely metal cube, to move in pure translation accurately in the purpose of obtaining a vanishing point of the structured light plane, and then the projection angle of the light plane projector was solved from the vanishing point, as well as the baseline, the intercept of structured light plane on *x*-axis of the image coordinate system. Yang et al.⁵ got two parallel lines on the structured light plane by using a 3D target with two precisely visible parallel planes, when several vanishing points were obtained, the normal vector of the structured light plane could be deduced. As the baseline was solved based on the invariance of cross-ratio, calibration of the structured light plane was accomplished. Unfortunately, 3D target based method^{6–8} is not accurate enough because of the problem of mutual occlusion between different planes of the target and fewer feature points. Additionally, the 3D target, normally a cube with some special accessories, is difficult to make precisely and cumbersome for on-site calibration.

The planar target based method is more available to calibrate *LSLVS*. Wei et al.^{9,10} utilized a planar target with checkerboard pattern to finish the calibration. Based on the invariance of double cross-ratio, intersection points of the light stripe and checkerboards can be obtained under the image coordinate system as the exactly known size of each checkerboard. Then enough feature points on the light plane can be obtained. According to related fitting algorithm, expression of the light plane under the camera coordinate system can be calculated out. Liu et al.¹¹ proposed a new method according to Plücker matrix to represent the light stripe on a planar target. When the target is located in several different positions, Plücker matrixes of light stripes can be obtained. Then

School of Science, Qingdao University of Technology, Qingdao 266520, China. email: shww@qtech.edu.cn

expression of the light plane can be solved by combining obtained Plücker matrixes. Wei et al.¹² calibrate a LSLVS based on vanishing feature. Vanishing points of the light plane could be obtained from intersection point of the light stripe and vanishing line of the target plane. Once the planar target is moved to enough different positions, the normal vector of the light plane could be calculated out as well as the vanishing line. As the size of the planar target is exactly known, the parameter D could be deduced consequently. Then function of the light plane under camera coordinate system was determined.

Compared with 3D target based method and planar target based method, 1D target based method¹³ is proposed owing to its convenient operation. Normally, feature points on the light plane can be obtained based on related algorithm, such as the intersection point of the light stripe and a 1D target, which can be obtained based on the invariance of cross-ratio. By moving the 1D target randomly to more different positions, enough feature points can be obtained to fit the light plane.

As the relative relation between the sensor and the laser projector is not request strictly as the sensor in the first category, this kind of sensor is cheap and convenient. Unfortunately, captured images over the whole measurement range are not sharp enough to get a precise measurement result, especially in the z -direction (height direction). In other words, measurement range of this kind of LSLVS in height direction is limited.

In the second category, relationship between the image sensor and laser projector satisfies the *Scheimpflug* condition strictly¹⁴, i.e., the CCD plane, the lens plane and the focus plane (normally a laser plane) intersect in a single line, which is named as *Scheimpflug* line. In this case, measurement range is enlarged. As requirement of the precise machining, this kind of LSLVS is expensive which is often utilized as a commercial sensor such as *KEYENCE LJ-X8000*, *COGNEX DS910B* and so on. Moreover, calibration method is difficult for this kind of LSLVS. Shao et al.¹⁵ give a mathematic model to define the camera with a tilted lens. Then the measurement mode for the LSLVS in *Scheimpflug* conditions is given. When the target with circle pattern is located in the measurement range, the LSLVS can be calibrated. But as the location/pose of the target is limited, precision of the calibration is not high enough.

So how to enlarge the measurement range and execute an easy calibration method to get precise measurement results are significant, which are also the purpose of all kinds of 3D laser scanners. In this work, we propose a measurement method for the LSLVS in traditional construction, including its calibration method. Compared with a traditional measurement method, distortion compensation is not necessary and precision of measurement is improved significantly. Moreover, this approach can also be used to the LSLVS in *Scheimpflug* conditions.

Model of a LSLVS

LSLVS in traditional structure. A typical structure of a LSLVS in traditional structure is illustrated in Fig. 1a, while its corresponding measurement model is in Fig. 1b. As illustrated in Fig. 1a, a laser projector projects a laser stripe onto surface of the measuring object. Images of the laser stripe are captured by the camera. According to the measurement model (which is illustrated in Fig. 1b), 3D coordinates of feature points on the laser plane under the camera coordinate system can be calculated out.

In Fig. 1b, O -XYZ is the Camera Coordinate System (CCS) while o - xy is the Image Coordinate System (ICS). Under the CCS, center of the camera is at the origin and the optical axis points to the positive Z direction. A spatial point P is projected onto the plane with $Z=f_0$, referred to as the image plane under the CCS, where f_0 is the effective focal length (EFL). Supposing $p=(x, y, 1)^T$ is the projection of $P=(X, Y, Z)^T$ on the image plane. Under the idealized pinhole imaging model, P , p and center of the camera O are collinear. Relationship between the camera and the laser projector remains unchangeable in the process of measurement¹².

Traditionally, determining the relationship (i.e. mathematical expression of the laser plane under the CCS) is very important which is known as calibration of a LSLVS.

LSLVS in Scheimpflug conditions. Imaging model of a *Scheimpflug* camera can be illustrated by Fig. 2. The O_C - X_C Y_C Z_C is CCS while the o - xy is the ICS which is parallel with the lens plane. Meanwhile, we can obtain a 3D coordinate system o - xyZ_c . When the lens is tilted, o - xyZ_c is transformed to o - XYZ . The transformation

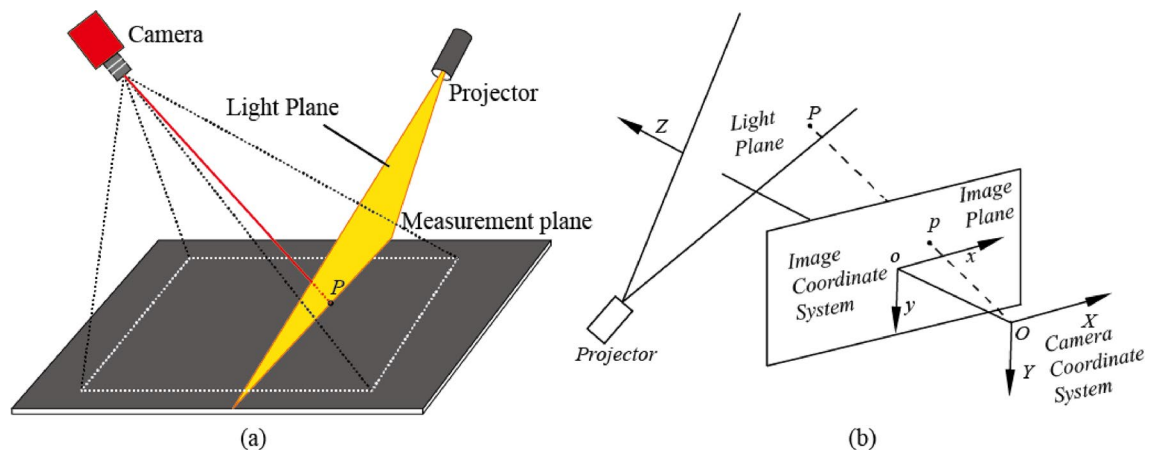


Figure 1. (a) The typical structure of a LSLVS and (b) its measurement model.

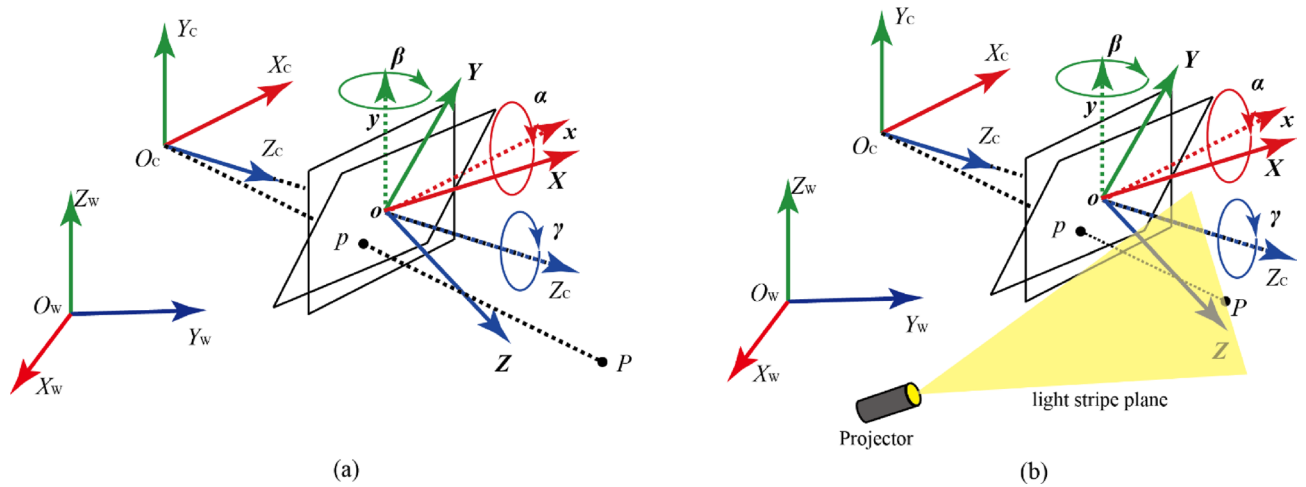


Figure 2. (a) Imaging model of a *Scheimpflug* camera, (b) Measurement model of a *LSLVS* in *Scheimpflug* conditions.

matrix can be defined as R . Under *CCS*, the camera center is at the origin and the original optical axis points in the positive Z_c direction. When the lens is tilted, the optical axis is transformed to Z direction. A spatial point P is projected to the plane o - XY , referred to as the real image plane under *CCS*. f_0 ($|oO_c|$) is the effective focal length (*EFL*). Supposing $p = (x, y, 1)^T$ is the projection of $P = (X, Y, Z)^T$ on the image plane. Under the idealized pinhole imaging model, i.e. the ideal model of the camera, P , p and the camera center O are collinear^{14,16}.

For the related *LSLVS*, structure satisfies the *Scheimpflug* condition, i.e., the image plane, the lens plane and light plane intersect in the *Scheimpflug* line theoretically. As is known, expression of the lens plane under the *CCS* is the Z -plane. The light plane can be expressed as

$$s_\beta c_\alpha X - s_\beta Y + 2c_\beta c_\alpha Z - c_\beta c_\alpha f = 0 \tag{1}$$

where $c_\theta = \cos \theta$ and $s_\theta = \sin \theta$. α is the rotation angle around x -axis, while β is the rotation angle around y -axis and γ is the rotation angle around z -axis.

Related method

Feature points on planar target. As is known, the most commonly used planar target is with a checkerboard pattern, which is used to calibrate the camera intrinsic parameters using *Zhang's* method¹⁷. When a laser stripe projected on the target, we can get the intersection of light stripe and side of each checker on the image plane (as point D and point D_1 in Fig. 3).

As the side length of each checkerboard is known exactly, the coordinate of the feature points under target coordinate system (*TCS*) can be solved based on the invariance of cross-ratio. The theory is described as follow:

The grid pitch of the target is known accurately as l while the length of AD can be defined as l_0 (see Fig. 3). Based on the invariance of cross-ratio, the following equation can be obtained:

$$\frac{AB/BD}{AC/DC} = \frac{2l/(2l - l_0)}{3l/(3l - l_0)} \tag{2}$$

The real length of AD can be solved, so can A_1D_1 . Then the distance between point D and point D_1 can be worked out. In this case, coordinates of point D and point D_1 under *TCS* can be confirmed. Moreover, any one of feature points between point D and point D_1 can be calculated out according to related interpolation algorithm.

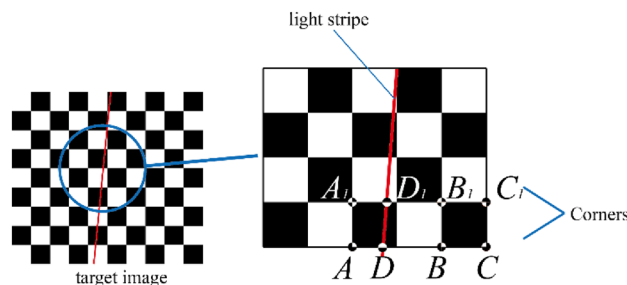


Figure 3. Determination of feature points on planar target.

Steger’s extraction algorithm. Steger’s algorithm is an extraction algorithm with a sub-pixel precision. It can be used to extract the centerline of a curvilinear structure, such as a laser stripe.

Define the 2D gray-value distribution function of the image as $I(X, Y)$, where (X, Y) are the coordinates of the image point. The variable quantity of gray values in the position of (X, Y) is defined as Δ while the change of direction is defined as n . n and Δ can be determined by Hessian Matrix of $I(X, Y)$. The Hessian Matrix is defined as¹⁸

$$Hess(I(X, Y)) = \begin{bmatrix} I_{XX} & I_{XY} \\ I_{XY} & I_{YY} \end{bmatrix} \tag{3}$$

where *Hess* indicates numeration of a Hessian Matrix, and the other related notations are defined as below:

$$\begin{cases} I_{XX} = I(X, Y) \otimes g_{xx}(x, y) \\ I_{XY} = I(X, Y) \otimes g_{xy}(x, y) \\ I_{YY} = I(X, Y) \otimes g_{yy}(x, y) \end{cases}, \tag{4}$$

In Eq. (4), g_{xx} , g_{xy} and g_{yy} are the second-order differential discrete Gaussian convolution kernel and \otimes denotes the calculation of convolution. These two eigenvalues of the Hessian Matrix denote the maximum and the minimum of the second derivative of $I(X, Y)$. In other words, the eigenvalues of the Hessian Matrix indicate variation in directions of the acutest change and the smoothest change and their corresponding eigenvectors are the related directions.

The centerline of the curvilinear structure is the position where its first-order derivative is zero. Then the center of the curvilinear structure can be determined with sub-pixel accuracy by the second-order Taylor expansion gray-value distribution function. The center with sub-pixel accuracy can be expressed as:

$$(p_x, p_y) = (tn_x + x_0, tn_y + y_0), \tag{5}$$

where

$$t = -\frac{n_x g_x + n_y g_y}{n_x^2 g_{xx} + 2n_x n_y g_{xy} + n_y^2 g_{yy}}, \tag{6}$$

(x_0, y_0) is the center with pixel accuracy, whose direction is determined by the eigenvector of the Hessian Matrix, g_x and g_y are the first-order partial derivative of the gray-value distribution function in position (x_0, y_0) , while g_{xx} , g_{xy} , g_{yy} are the second-order partial derivatives of the gray-value distribution function in position (x_0, y_0) ¹⁹

Normalized feature points in one direction. When we extract center points of line structure feature (such as light stripe and so on) on the image plane with a sub-pixel precision, coordinates of feature points are not a whole number. In some case, *x*-coordinate/*y*-coordinate of feature point should be normalized to a whole number. This process is named as normalization of feature points in *x*-direction/*y*-direction in this paper.

Define point $I(x, y)$ is the extracted feature point of line structure, point $A(x_A, y_A)$ is the closest point to I on the left, while point $B(x_B, y_B)$ is the closest point to I on the right. When we normalized point I in *x*-direction, we can get coordinates as

$$(x_{norm}, y_{norm}) = (x_{round}, \frac{(y_B - y_A)x_{round} + y_A x_B - y_B x_A}{x_B - x_A}) \tag{7}$$

Moreover, when we normalized point I in *y*-direction, we can get coordinates as

$$(x_{norm}, y_{norm}) = (\frac{y_{round}(x_B - x_A) - y_A x_B + y_B x_A}{y_B - y_A}, y_{round}) \tag{8}$$

Relation between feature point and distance. When obtained enough feature points in different distances, relation between feature point and the distance can be worked out. Once enough sample points are obtained, we can get the relation according to several algorithms, such as curve fitting algorithm, Back-Propagation (BP) neural network algorithm and so on.

① Adaptive curve fitting algorithm

In this section, we use a linear function and a second order function to approximate the relationship. Procedure is detailed as follow:

Step. 1. Define a linear function as

$$f(x) = ax + b \tag{9}$$

and a second order function as

$$g(x) = ax^2 + bx + c \tag{10}$$

Step. 2. Normalized feature points and selected feature points with the same x -coordinate/ y -coordinate as the x value. Its corresponding distance is chosen as the y value.

Step. 3. Using least square fitting method²⁰ to calculate coefficients a and b in Eq. (9). If value of the objective function ε (Eq. 11) is smaller than a threshold (such as $1e-4$), coefficients are saved and the linear function is selected as the function to express the relation. Else, go to Step.4.

$$\varepsilon = \sum_{i=0}^N |f(x_i) - y_i|^2 \quad (11)$$

In Eq. (11), $f(x)$ is defined as Eq. (9), x_i is the normalized x -coordinate/ y -coordinate, while y_i is corresponding real distance.

Step. 4. Using least square fitting method to calculate coefficients a , b and c in Eq. (10). If value of the objective function κ (Eq. 12) is smaller than ε , the second order function is selected as the function to express the relation.

$$\kappa = \sum_{i=0}^N |g(x_i) - y_i|^2 \quad (12)$$

In Eq. (12), $g(x)$ is defined as Eq. (10), x_i and y_i are defined the same as in Eq. (11).

② BP neural network algorithm²¹

In this section, a BP neural network with three layers is chosen to obtain the relation between feature point and distance.

Step. 1. Normalized feature points and selected feature points with the same x -coordinate/ y -coordinate as the x value. Its corresponding distance is chosen as the y value.

Step. 2. Initialize BP neural network. Select connection weights and thresholds randomly.

Step. 3. According to related algorithm for input and output, re-calculate the output values of hidden layer and output layer. Then update related weights and thresholds.

Step. 4. Repeat until the error is less than threshold. Then we can get the relation between feature point and distance.

Calibration procedure

In traditional calibration method, expression of the laser plane under CCS should be obtained. But when these captured images are not sharp enough, the calibration results will involve more error. In this section, a new calibration is proposed, including getting the relationship between image point and horizontal distance and the relationship between image point and perpendicular distance. This calibration method is suitable for both LSLVSs in traditional structure and in *Scheimpflug* conditions.

Preparation. *Step. 1.* Select a suitable linear translation stage. As is known, positional precision of a linear translation stage is high enough to calibrate any one laser scanner. In this case, we can choose a suitable linear stage according to the accuracy requirement of our LSLVS.

Step. 2. Machine a surface plate with a proper precision. As the plate is not with any pattern or 3D feature, productive process is not difficult.

Step. 3. A LSLVS in traditional structure includes a camera with normal lens and a laser projector. The sensor is fixed on a rigid beam. In this case, the relationship between the camera and the laser projector is unchangeable.

For perpendicular distance. *Step. 1.* Fix our LSLVS on the stage. In this case, the LSLVS can move up and down along the moving direction of the linear translation stage. The translation value is same with the stage, which is easy to obtain.

Step. 2. Place the surface plate under the laser projector to cover the measurement range and fix. In this case, image of the laser stripe on the plate can be captured by the camera.

Step. 3. Control the linear translation stage moving within the longitudinal measurement range with a fixed step, which is normally equal to the measurement resolution. Capture one image of light stripe for each position.

Step. 4. Extract center points of light stripe in each image. In this paper, the extraction method is Steger's extraction algorithm¹⁹ with a precision of subpixel.

Step. 5. Normalized image feature points. Then get the function between coordinate of center points and perpendicular distance in each position according to related method.

For horizontal distance. *Step. 1.* Fix our LSLVS on the stage. In this case, the LSLVS can move up and down along the moving direction of the linear translation stage.

Step. 2. Place a planar target with checkerboard-pattern on the surface plate.

Step. 3. Control the linear translation stage moving within the longitudinal measurement range with a fixed step. Then capture one image of light stripe (with the planar target) for each position.

Step. 4. Extract center points of light stripe in each image. In this paper, the extraction method is Steger's extraction algorithm¹⁹ with a precision of subpixel.

Step. 5. Normalized image feature points according to normalization algorithm mentioned in Part B of Section III. Then get the function between coordinate of center points and horizontal distance in each position according to related method.

System structure

The structure of our experiment apparatus is illustrated in Fig. 4. For simplicity, we built a LSLVS with a traditional structure in our work, which includes a camera with a normal lens and a laser projector (Note that a LSLVS in *Scheimpflug* condition can also be utilized). The sensor is fixed on a rigid beam. In this case, the relationship between the camera and the laser projector is unchangeable. Then the beam is fixed on a linear translation stage. Components are detailed as following.

LSLVS. The camera used in our LSLVS is *DaHeng MER-1070-10GM-P* with a resolution of 3840×2748 pixels while the laser projector is with a wavelength of 405 nm. In practice, the resolution in x -direction is reduce to 3300 pixels to make sure a whole light stripe is captured. Baseline between the camera and the laser projector is about 500 mm. As the focal length of our lens is 6 mm, measurement range is about 1100 mm while the nearest perpendicular distance from the rigid beam to the reference plane is about 800 mm.

Linear translation stage. The stage used to calibrate the LSLVS is chosen as PST150 X-S42 with a stroke of 150 mm. Resolution of the stage is 2.5 μs , while the repositioning precision is 4 μs . Positional accuracy of the linear translation stage is with a high enough precision according to the measurement requirement of the LSLVS. As the measurement range is 1100 mm, we selected the aimed precision as 0.1 mm, i.e., 0.09‰ relative to the measurement range, which is better than most existing sensors in *Scheimpflug* conditions.

Surface plate. Precision of the planeness is 0.05 mm and the length is 1200 mm. As the plate is not with any pattern or 3D feature, precise machining is easy to finish. In the process of calibration, the LSLVS projects a laser stripe onto the surface plate, and the camera captures images of the laser stripe.

Planar target. The planar target used to get feature points on light stripe is with a checkerboard pattern (as illustrated in Fig. 5). Machining precision of the planar target is 5 μm . The side length of each checkerboard is 25 mm. The surface of the planar target is diffusely reflected. In this case, feature points on light plane can be obtained easily.

Experiments and discussion

Camera calibration. With the help of the planar target mentioned above, camera used in the system is calibrated by *Zhang's* calibration method¹⁷. In this method, the target is located in camera's field of view randomly. In this case, images of the target can be captured by the camera sharply. When the target is located into more than three different positions with different poses, the camera can be calibrated successfully. In our paper, sixteen images are captured to finish the calibration task and part of images are illustrated in Fig. 6.

Obtained intrinsic parameters are listed in Table 1.

In Table 1, f_x and f_y are scale factors in x -coordinate and y -coordinate, and (u_0, v_0) are the principal point of the image plane. kc_1 and kc_2 are distortion factors of the image.

Calibration of LSLVS. In the calibration for our LSLVS, the fixed step of the linear translation stage is 0.1 mm while the longitudinal measurement range is 100 mm. In this case, we should capture 1001 images to get the relation between feature points and perpendicular distance. Then the planar target is located on the



Figure 4. Construct of our experiment apparatus.

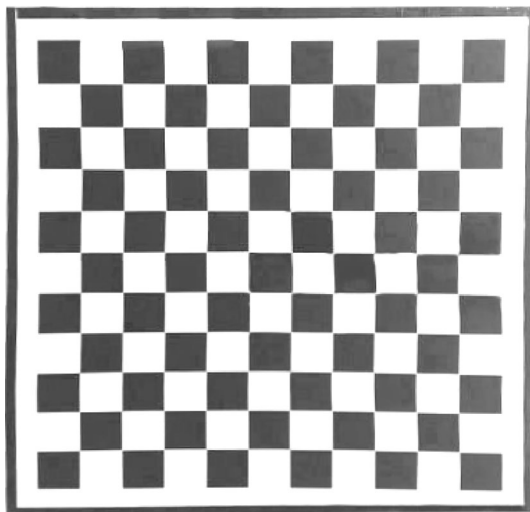


Figure 5. The planar target with checkerboard pattern.

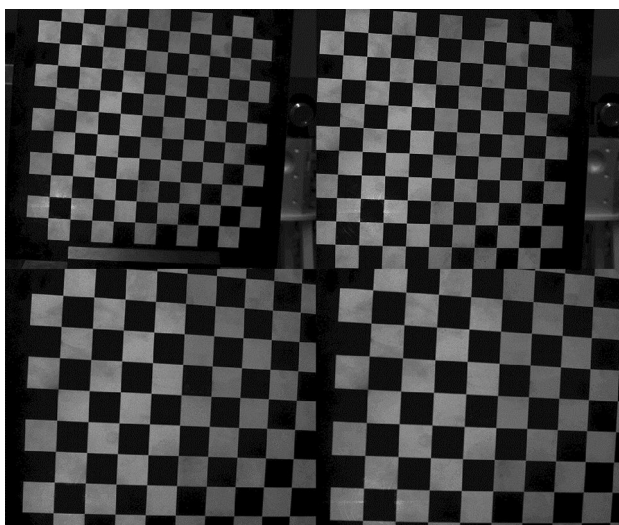


Figure 6. Part of target images used to calibrate the camera.

f_x	f_y	u_0	v_0	kc_1	kc_2
3744.76	3754.28	1625.68	223.19	-0.130	0.026

Table 1. Intrinsic parameters of the camera in our system.

surface plane to get the relation between feature points and horizontal distance. For each image, the light stripe is extracted by Steger's method¹⁹ and then feature points are normalized by method mentioned in Section II.

As the resolution of the image on x -direction is 3300, we should get 3300 functions to express relationship for each pixel in whole measurement range. Relationship between distance and coordinate of laser stripe are illustrated in Fig. 7a. As illustrated in Fig. 7a, each column is variation of distance with the same x -coordinate of feature points. In other words, each column denotes function of distance with y -coordinate. Sample of relationship between the y -coordinate and the distance in one position of the laser stripe is illustrated in Fig. 7b. From Fig. 7b, the relationship can be confirmed by two algorithms, i.e., the adaptive curve fitting algorithm and BP neural network algorithm. In the adaptive curve fitting algorithm, the each relationship (as plotted in Fig. 7b) is fitted by a linear function as Eq. (9) or a second order function as Eq. (10), while in the BP neural network algorithm the relationship of input and output is expressed by a trained network model.

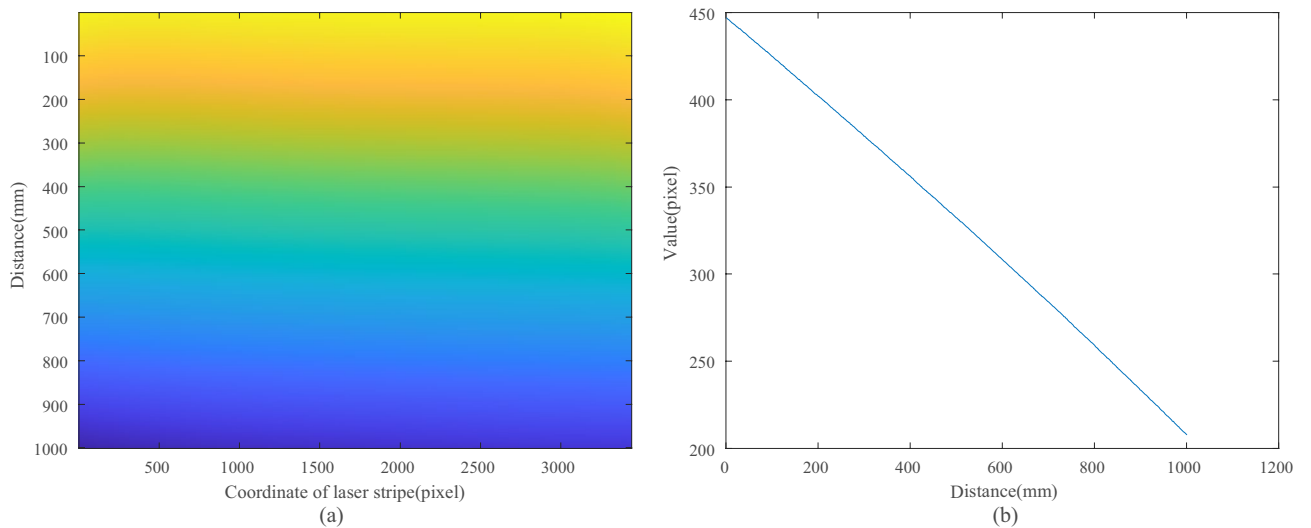


Figure 7. (a) relationship between distance and coordinate of laser stripe; (b) relationship between the value and the distance in one position of the laser stripe.

Evaluations.

① For perpendicular distance

In order to evaluate the measurement precision of the *LSLVS* in perpendicular direction according to our proposed approach, we produce a step wedge with a precision of 0.02 mm. Heights of these step surfaces are 10.0 mm, 19.0 mm, 27.9 mm and 32.5 mm respectively. The wedge is located on a surface plate. These measurement results are illustrated as Fig. 8. From these measurement results we can get maximum of the error as 0.1 mm. As the fixed step of the linear translation stage used to get the relationship is 0.1 mm, measurement precision of our laser scanner is precise enough.

② For horizontal distance

A 1D target which is illustrated in Fig. 9, is used to evaluate the measurement precision of the laser scanner in horizontal direction. The distance between each two adjacent feature points is known exactly (40 mm). All measurement values are compared with their corresponding true value. As the target can be moved into different positions randomly, we can obtain enough distances to evaluate our measurement method in horizontal direction. Part of our evaluation results are listed in Table 2. In Table 2, D_{m1} denotes the measurement result according to adaptive curve fitting algorithm, while D_{m2} denotes measurement result according to BP neural

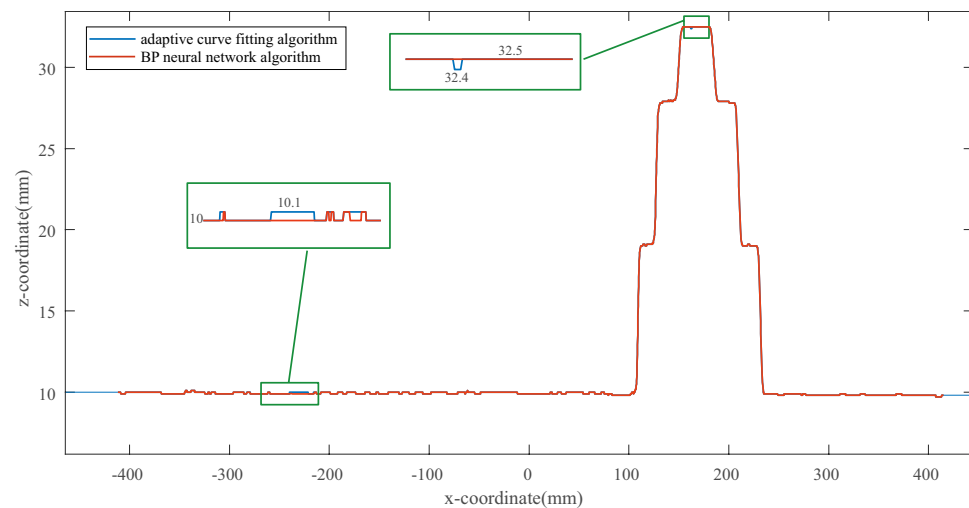


Figure 8. Measurement results to evaluate the measurement precision of our LSLVS.



Figure 9. 1D target to evaluate our measurement method in horizontal direction.

No	D_{real}	D_{m1}	D_{m2}	Error1	Error2
1	40.00	40.08	40.06	0.08	0.06
2	40.00	39.92	39.93	- 0.08	- 0.07
3	40.00	39.90	39.92	- 0.10	- 0.08
4	40.00	39.97	39.95	- 0.03	- 0.05
5	40.00	40.05	40.06	0.05	0.06
6	40.00	39.96	39.97	- 0.04	- 0.03
7	40.00	40.03	40.04	0.03	0.04
8	40.00	39.96	39.98	- 0.04	- 0.02
9	40.00	39.91	39.96	- 0.09	- 0.04
10	40.00	40.06	40.04	0.06	0.04
RMS				0.065	0.052

Table 2. Result of the evaluation (unit:mm).

network algorithm. Correspondingly, Error1 is the absolute error of D_{m1} and Error2 is the absolute error of D_{m2} . As listed in Table 2, the root mean square error (RMS error) of measurement results according to our proposed method is 0.065 mm (according to adaptive curve fitting algorithm) and 0.052 mm (according to BP neural network algorithm).

Comparison. For comparison, we calibrate the *LSLVS* using Wei's calibration method^{9,10}. The expression under *CCS* of the light plane is

$$-0.014X - 0.793Y + 0.608Z - 581.157 = 0 \quad (13)$$

we measure the 1D target illustrated in Fig. 8 according to the traditional method (D_{trad}) and our proposed method (D_{m1} and D_{m2}). The measurement results are listed in Table 3.

As listed in Table 3, RMS error of measurement results according to the traditional method is 0.184 mm, which is at least reduced by 64.67%.

Conclusion

In this paper, we propose a precise measurement method for a line structure light vision sensor, including corresponding calibration method. Related procedure is detailed in this paper. Compared to a traditional measurement method, distortion compensation is not necessary and precision of measurement is improved. Moreover, we demonstrated the error of our present measurement method in a large measurement range (about 1100 mm) is 0.1 mm, i.e., 0.09‰ relative to the measurement range. Real experiments show that root mean square error of measurement results according to our proposed method is reduced by 64.67% related to the traditional method. Moreover, our proposed method can also be used for the line structure light vision sensor in *Scheimpflug* conditions.

No	$D_{\text{real}}(\text{mm})$	D_{m1}	D_{m2}	$D_{\text{trad}}(\text{mm})$
1	40.00	40.08	40.06	40.15
2	40.00	39.92	39.93	40.11
3	40.00	39.90	39.92	39.82
4	40.00	39.97	39.95	39.93
5	40.00	40.05	40.06	40.20
6	40.00	39.96	39.97	39.78
7	40.00	40.03	40.04	39.83
8	40.00	39.96	39.98	39.75
9	40.00	39.91	39.96	40.24
10	40.00	40.06	40.04	40.17
RMS		0.065	0.052	0.184

Table 3. Comparison results of measurement.

Data availability

All data generated or analysed during this study are included in this published article.

Received: 7 October 2022; Accepted: 29 April 2023

Published online: 04 May 2023

References

- Sun, J., Zhang, J., Liu, Z. & Zhang, G. J. A vision measurement model of laser displacement sensor and its calibration method. *Opt. Laser Eng.* **51**, 1344–1352 (2013).
- Shao, M. W. & Hu, M. J. Parallel feature based calibration method for a trinocular vision sensor. *Opt. Express* **28**(14), 20573–20586 (2020).
- Heikkila, J. Geometric camera calibration using circular control points. *IEEE Trans. Pattern Anal. Mach. Intell.* **22**(10), 1066–1073 (2000).
- Xiao, H. & Luo, M. A line structured light 3D visual sensor calibration by vanishing point method. *Opt.-Electron. Eng.* **23**(3), 53–58 (1996).
- Yang, P. & Lin, Wu. A rapid calibration method for laser light vision sensor. *Laser J.* **27**(4), 35–36 (2006).
- Duan, F., Liu, F. & Ye, S. A new accurate method for the calibration of line structured light sensor. *Chin. J. Sci. Instrum.* **21**(1), 108–110 (2000).
- Zou, D., Research on 3D vision inspection and its application in ADC station. [Ph.D. Dissertation], Tianjin University (1992).
- Zhang, S. & Huang, P. S. Novel method for structured light system calibration. *Opt. Eng.* **45**, 8. <https://doi.org/10.1117/1.2336196> (2006).
- Wei, Z. & Zhang, G. Calibration approach for structured-light-stripe vision sensor based on the invariance of double cross-ratio. *Opt. Eng.* **42**(10), 2959–2966 (2003).
- Zhou, F. & Zhang, G. Complete calibration of a structured light stripe vision sensor through planar target of unknown orientations. *Image Vis. Comput.* **23**(1), 59–67 (2005).
- Liu, Z., Zhang, G. & Wei, Z. An accurate calibration method for line structure light vision sensor. *Acta Opt. Sin.* **29**(11), 3124–3128 (2009).
- Wei, Z. Z., Shao, M. W., Zhang, G. J. & Wang, Y. L. Parallel-based calibration method for line-structured light vision sensor. *Opt. Eng.* **53**(3), 033101 (2014).
- Wei, Z., Cao, L. & Zhang, G. A novel 1D target-based calibration method with unknown orientation for structured light vision sensor. *Opt. Laser Technol.* **42**, 570–574 (2010).
- Scheimpflug, T. Improved method and apparatus for the systematic alteration or distortion of plane pictures and images by means of lenses and mirrors for photography and other purposes. Great Britain Patent 1196 (May 12, 1904).
- Shao, M. W. Calibration methods for a camera with a tilted lens and a three-dimensional laser scanner in the Scheimpflug condition. *J. Opt. Soc. Am. A. Opt. Image. Sci. Vis.* **37**(7), 1076–1082 (2020).
- Shao, M. W., Wang, P. & Wang, J. H. Improved sensors based on scheimpflug conditions and multi-focal constraints. *IEEE ACCESS* <https://doi.org/10.1109/ACCESS.2020.3020731> (2020).
- Zhang, Z. A flexible new technique for camera calibration. *IEEE Trans. Pattern Anal. Mach. Intell.* **22**(11), 1330–1334 (2000).
- Shao, M., Wei, Z., Hu, M., A flexible method for calibrating external parameters of two cameras with no-overlapping FOV. In *Seventh International Symposium on Precision Mechanical Measurements*, ID:99032C (2016).
- Steger, C. Unbiased extraction of lines with parabolic and Gaussian profiles. *Comput. Vis. Image Underst.* **117**, 97–112 (2013).
- Zhang, L. et al. An adaptive moving total least squares method for curve fitting. *Measurement* **49**, 107–112 (2014).
- Yip, H. J., Ji, G. R., Liu, J. H., Jia, L., Optimal structure and parameters of BP neural network for curve fitting problem. The 6th EMIM, vol. 40, pp. 1647–1652 (2016).

Acknowledgements

This research was funded by Natural Science Foundation of Shandong Province (ZR2022ME182), China.

Author contributions

W.S. wrote the main manuscript text, prepared figures and reviewed the manuscript.

Competing interests

The author declares no competing interests.

Additional information

Correspondence and requests for materials should be addressed to W.S.

Reprints and permissions information is available at www.nature.com/reprints.

Publisher's note Springer Nature remains neutral with regard to jurisdictional claims in published maps and institutional affiliations.



Open Access This article is licensed under a Creative Commons Attribution 4.0 International License, which permits use, sharing, adaptation, distribution and reproduction in any medium or format, as long as you give appropriate credit to the original author(s) and the source, provide a link to the Creative Commons licence, and indicate if changes were made. The images or other third party material in this article are included in the article's Creative Commons licence, unless indicated otherwise in a credit line to the material. If material is not included in the article's Creative Commons licence and your intended use is not permitted by statutory regulation or exceeds the permitted use, you will need to obtain permission directly from the copyright holder. To view a copy of this licence, visit <http://creativecommons.org/licenses/by/4.0/>.

© The Author(s) 2023